Chaotic dynamics in the map model of fluxon propagation in long Josephson junctions

G. Rotoli and G. Filatrella

Department of Physics, University of Salerno, I-84081 Baronissi (SA), Italy

Received 20 November 1990; revised manuscript received 20 March 1991; accepted for publication 18 April 1991
Communicated by A.P. Fordy

Chaotic dynamics in a model of a long Josephson junction (LJJ) is studied via standard techniques of non-linear maps. A characterization of chaos in such objects in terms of Lyapunov exponents and Poincaré sections is given. Finally the occurrence of chaos in map dynamics is compared with preliminary results of full numerical integration of the perturbed sine-Gordon equation (PSGE).

The partial differential equation (PDE) modeling a long Josephson junction (LJJ) [1–3] is a typical example of an equation sustaining solitonic solutions. Such solitons, called fluxons because they carry a flux quantum $h/2e$, are characterized by a high spatial coherency over a length of λ_J, i.e. the Josephson length. On the other hand the occurrence of chaotic states in the differential equations modelling ac driven small [4,5] and long [6,7] Josephson junctions is a well known phenomenon. Recently, also in the context of a simplified model of a LJJ which reduces the problem to the study of a two-dimensional functional map evidence of chaotic states has been shown [8,9]. The features of this last result are remarkable because they involve both aspects: solitons and chaotic behavior [9]. The pseudo-random evolution in deterministic systems is of great interest from a theoretical point of view, but also from an applicative one in order to avoid a possible source of noise in practical devices.

Small junctions can be modelled by a non-linear ordinary differential equation for $\phi(t)$, the phase difference between the two superconductors which form the junction. When junctions are in the presence of an external rf signal they can, under suitable conditions, show chaotic behavior, i.e. the phase relation of $\phi(t)$ with the external rf signal is chaotic.

Long Josephson junctions [1] are described by a non-linear partial differential equation with proper boundary conditions. The solution of this equation is again the phase $\phi(x, t)$. This equation can be written, in normalized units, for an inline junction irradiated by a microwave field as

$$\phi_{tt}-\phi_{xx}+\sin\phi=\alpha\phi_t-\beta\phi_{xxt}\,, \tag{1}$$

where α and β are, respectively, the quasi-particle loss and the surface loss. Boundary conditions are (l is the normalized length of the junction)

$$\phi_x(0,t)+\beta\phi_{xt}(0,t)=-\chi+\eta_0\sin(\omega t)\,, \tag{2a}$$

$$\phi_x(l,t)+\beta\phi_{xt}(l,t)=\chi+\eta_0\sin(\omega t) \tag{2b}$$

to take into account the effect of both the dc drive χ and of an oscillating external magnetic field $\eta(t)=\eta_0\sin(\omega t)$ [8–12] (in normalized units). This equation can sustain the motion of localized kinks, called also fluxons because they carry a flux quantum trapped in a 2π rotation of the phase.

Under suitable conditions, assuming that only a single fluxon is present in the junction, it is possible by means of a perturbative approach to reduce eq. (1) to an ordinary differential equation for the velocity $u(t)$ of the center of mass of the fluxon [13]. This differential equation has been used to write a two-dimensional functional map. The map has been discussed elsewhere (see refs. [8–10] for a complete discussion), and here it is written in terms of the variables t_k (the time variable of the soliton, modulo the period of the external signal, after the kth reflection at a boundary) and u_k (the velocity at the kth boundary),

$$t_{k+1}=t_k+\frac{1}{a}\ln\left(\frac{u_k}{Cu_k-S_\lambda}\right)\quad \mathrm{mod}(2\pi/\omega)\ , \tag{3a}$$

$$u_{k+1}=\sqrt{1-1/y_{k+1}^2}\ , \tag{3b}$$

where y_k, the fluxon energy at the kth reflection, is

$$y_{k+1}=\sqrt{\frac{(1-\lambda)(Cu_k-S_\lambda)^2+1-(1-\lambda)u_k^2}{1-(1-\lambda)u_k^2-\lambda(Cu_k-S_\lambda)^2}}$$

$$+\tfrac{1}{2}\pi[\chi+(-1)^k\eta_0\sin(\omega t_k+\theta)]\ , \tag{3c}$$

where $a=\alpha+\frac{1}{3}\beta$, $C=\cosh(al\sqrt{1-\lambda})$, $S_\lambda=\sinh(al\sqrt{1-\lambda})/\sqrt{1-\lambda}$, $\lambda=\frac{1}{3}\beta/(\alpha+\frac{1}{3}\beta)$. We note that from eq. (3a) we can obtain the time of flight (TOF) of a soliton defined as $T_{k+1}=t_{k+1}-t_k$, i.e. the time employed by the fluxon to propagate between the ends of the LJJ. Thus the general condition for the existence of single fixed point phase-locked states is

$$T_k+T_{k+1}=\frac{m}{n}\frac{2\pi}{\omega}\ , \tag{4a}$$

$$u_{k+p}=u_k\ , \tag{4b}$$

where m, n and p are integers. These phase-locked states give rise to vertical steps on the current–voltage (I–V) characteristic, i.e. the voltage, proportional to the inverse of the TOF, remains constant in spite of the change of current. This effect has been experimentally observed [14,15]. A study of the stability of these states can be performed analytically by linearizing the map around the fixed points [10]. Here we are interested in the onset of chaos, which is not predictable a priori from the map. Numerical iteration of the map shows evidence of a chaotic regime (see fig. 1a). The control parameter is the external magnetic field η_0, which is proportional to the square root of the power of the microwave field. The current χ is taken always as the current value at the center of the induced step. The parameter η_0 was slowly raised from 0 to a value $\eta_0^{\rm a}$, when the fluxon is "annihilated". We say that the fluxon is annihilated if after the reflection the energy is less than the rest energy or not sufficient, because of dissipation, to cross the entire length of the junction [8]. Note

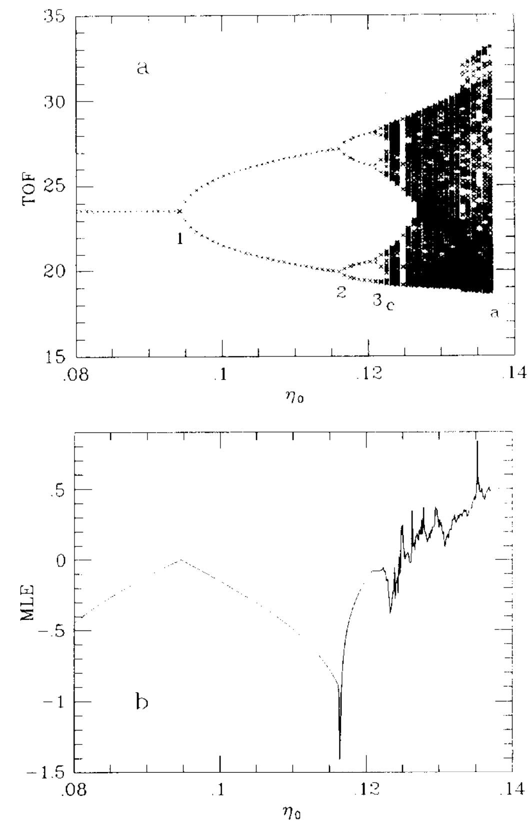

Fig. 1. (a) Bifurcation tree for map approach to LJJ of length $l=10$, $\alpha=0.1$, $\beta=0.025$, $\omega=0.4$, $\chi=0.574$ (corresponding to the central value of phase-locking zone); (b) maximum Lyapunov exponent (MLE) for the same bifurcation tree.

that we have plotted, to improve readibility, the TOFs T_k instead of the time t_k.

We denote by η_0^1 the values of the control parameter at the first instability which leads to two TOFs, and by $\eta_0^{\rm c}$ the value at onset of chaos. During the period-doubling cascade and in the chaotic regime the voltage, in these units given by $2\pi/\langle T_k\rangle_{\rm ave}$, does not change and the system remains, in spite of the strongly chaotic motion, frequency locked to the external source, i.e. the phase-locking step is again perfectly vertical on the I–V characteristic [4]. In the chaotic state it is necessary to be very careful in evaluating the above average; the bigger the control parameter, the longer must be the averaging time to obtain a stable value of the voltage.

We conclude that no visible effects can be observed on the I–V characteristic, as long as we utilize the perturbative approach, which means essentially small signal regime ($\eta_0<0.4$–0.5), so that experimental evidence of the chaotic motion in this case can be realized only by means of the study of the Fourier spectra.

An extensive study of the range of parameters for the occurrence of chaotic phenomena has shown that if $m=1$ in eq. (4a) (we have studied only $n=1$) the bifurcation parameter η_0 becomes very large ($\eta_0>0.5$–0.6). Numerical integration of the PSGE shows that for such high values the single fluxon hypothesis is no longer satisfied (large signal regime). Chaos and the presence of a single fluxon in the LJJ can appear in the case of subharmonic excitation. However, if m is bigger than 5, the annihilation of the fluxon occurs for very small values of η_0, and a numerical (and experimental) study becomes very difficult. Probably $m=3$ is the best compromise to perform a study of the chaotic motion.

In summary, a chaotic regime in the map and the PSGE simulations is favored if

(1) α and β are decreased;

(2) χ is closer to the center of the step;

(3) m is increased.

An intuitive explanation in terms of incommensurate frequency models [4] is inadequate to explain the observed phenomena. In fact the natural frequencies of the two "clocks", the frequency of fluxon motion without any applied signal and the frequency of the external drive, are exactly the same in the center of the step, where we have observed that chaotic motion first occurs.

To achieve a deeper comprehension of the nature of this phenomenon we will describe "phenomenological" aspects of chaos in LJJs in the map context taking advantage of its speed and simplicity.

One of the most fruitful dynamical quantities to manifest the global aspects of a dynamical system are Lyapunov exponents. They are defined as the limit [4]

$$\Lambda_i=\log \lim_{n\to\infty}\left(\text{eigenvalues of } \frac{J(T_n,u_n)}{(T_0,u_0)}\right), \tag{5}$$

where J is the Jacobian matrix. Lyapunov exponents are negative if the orbits are periodic and, in the case of two-dimensional maps, one (the so-called maximum Lyapunov exponent, MLE) becomes positive in the chaotic regime. In this case the positive exponent is responsible for the spreading of the points in the phase plane, and the negative one for the condensation on the so-called "strange attractor" [4].

To evaluate numerically the MLE we have used a standard method [16], results of which are shown in fig. 1b. The MLE can be compared with fig. 1a to observe that, as expected, it approaches zero at the bifurcations and becomes positive in the chaotic regime. Another interesting property of the Lyapunov exponents is that the sum $\Lambda_1+\Lambda_2$ of the two exponents is a measure of the rate of contraction of phase volume; for a dissipative system this rate should depend upon the loss parameters of the system. In the case $\beta=0$ we have found a nice analytic relation between the rate of contraction and the loss parameter α. In this case the Jacobian of the map at the fixed point is simply $|J|=\exp(-\alpha T_k)$; from the definition of the Lyapunov exponent it follows that

$$\Lambda_1+\Lambda_2=-\alpha T_k=-\alpha m\pi/\omega\,. \tag{6}$$

Since in the chaotic regime the average of TOFs is $m\pi/\omega$ we conjecture that this relation is still valid when the dynamics is chaotic. We conjecture too that small β has no remarkable effects. These conjectures are supported by direct numerical simulations on the entire interval $[0,\eta_0^{\mathrm{a}})$. Assuming that eq. (6) is valid it says also that the higher m, the greater the squeezing of the attractors in the phase plane. Consequently the appearance of very long TOFs can destroy the fluxon. This mechanism can explain why for m bigger than 5 the chaotic region is so "compressed" by the annihilation region. We note parenthetically that eq. (6) is analogous to eq. (8) in ref. [4] for small junctions.

In fig. 2 a typical Poincaré section is shown. When the system is still phase-locked the single fixed point lies within the attractor. Increasing the control parameter the Feigenbaum cascade appears, and again the points are on the attractor, which is present at the appearance of chaotic motion. A further increase of η_0 leads to the appearance of points with progressively longer TOFs; this seems to be responsible for the annihilation of the fluxon, but the exact nature of the relation is not clear.

Another fundamental aspect of strange attractors is their fractal dimension. We have evaluated the Hausdorff and the information dimension of those

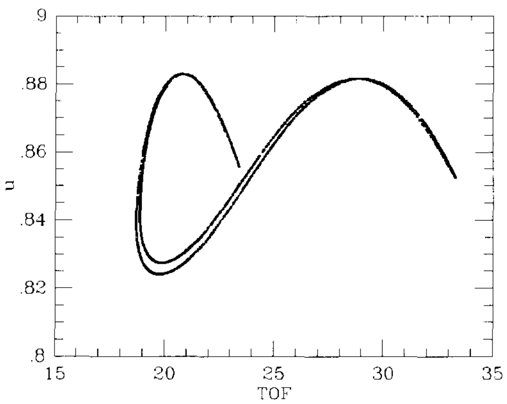

Fig. 2. Chaotic strange attractors for map approach to LJJ of length $l=10$, $\alpha=0.1$, $\beta=0.025$, $\omega=0.4$, $\eta_0=0.135$, $\chi=0.574$ (corresponding to the central value of phase-locking zone).

Table 1

η_0	Informatic dimension d_i	Hausdorff dimension d_H	Lyapunov dimension d_Λ
0.130	1.015 ± 0.018	1.067 ± 0.011	1.082 ± 0.005
0.131	1.052 ± 0.011	1.055 ± 0.010	1.055 ± 0.005
0.132	1.069 ± 0.017	1.069 ± 0.013	1.073 ± 0.005
0.133	1.111 ± 0.017	1.123 ± 0.016	1.108 ± 0.005
0.134	1.136 ± 0.014	1.134 ± 0.017	1.112 ± 0.005
0.135	1.133 ± 0.014	1.163 ± 0.015	1.162 ± 0.005

attractors with a direct measure in the phase plane dividing the phase plane $[0\times1]\times[0\times2\pi]$ in a grid of $2^j\times2^j$ cells (the choice of an integer power of 2 was just the simplest one from a computational point of view), then the map was iterated N times to estimate the quantities (d_H is the Hausdorff dimension and d_i the information dimension)

$$d_i = \lim_{\epsilon\to0}\left(-\sum_n \frac{P(\epsilon,n)\log P(\epsilon,n)}{\log(1/\epsilon)}\right), \tag{7}$$

$$d_H = \lim_{\epsilon\to0}\frac{\log N(\epsilon)}{\log(1/\epsilon)}, \tag{8}$$

where $N(\epsilon)$ is the number of cells visited by the system and $P(n,\epsilon)$ is the frequency at which the nth cell has been visited. Note that d_i cannot be bigger than d_H [17]. N was increased until a stable value of the dimension was reached; typical values are about $N=100000$. The procedure was repeated for several values of j and the resulting dimension was estimated extrapolating to $j\to\infty$ [18]. In table 1 are reported values of the Hausdorff and the information dimension and of the respective standard deviations as a function of the control parameter η_0 compared with the Lyapunov dimension defined as $d_\Lambda=1+\Lambda_1/|\Lambda_2|$ [4]. Under very general assumptions d_Λ should be bigger than the information dimension of attractors [17]. This is verified within an accuracy of two standard deviations. It seems that the Lyapunov dimension gives a reasonable estimation of the "brute-force" computed dimensions at a very low computational cost.

In fig. 3 we show the result of a full PSGE simulation of eq. (1). We have used a Burlish–Stoer method [19] with adaptive stepsize in time and a five-point approximation to the second derivative in space. For some parameter values it was compared with a simpler low-order predictor–corrector method [20] obtaining consistent results. Even if the scenario is very similar to those described above for the map it seems that the control parameter η_0 is less effective in producing instability in the PSGE system than it is in the map context. Nevertheless the similarity is evident and we have checked that also in the PSGE simulations the damping parameters can increase the stability [10]. For instance if β is set to zero in the case of fig. 1 the value of the first bifurcation η_0^1 and of the onset of chaos η_0^c are shifted by 20%. In spite of the different positions of the bifurcation tree the form of the PDE attractor is so reminiscent of the map attractor [21] that, in principle, a quantitative comparison between some of their

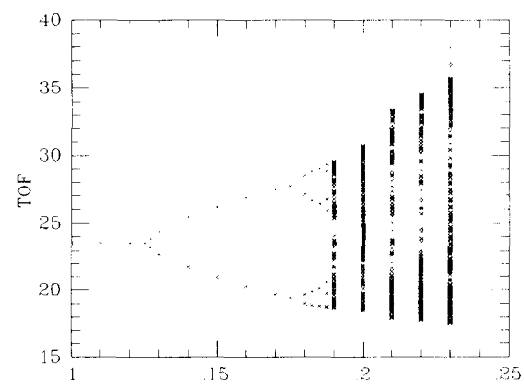

Fig. 3. Bifurcation tree for PSGE full model for a junction of length $l=10$, $\alpha=0.1$, $\beta=0.025$, $\omega=0.4$, $\chi=0.543$ (corresponding to the central value of phase-locking zone).

features, such as the fractal dimension, is possible. The direct comparison between the PDE and the map approach to verify the conjecture (6) for the PDE is very difficult because initial conditions (an essential ingredient to study the phase space) in terms of the collective coordinates are not suitable initial conditions for the PDE. The Feigenbaum universal ratio

$$\delta = \lim_{k\to\infty} \frac{\eta_0^{k+1} - \eta_0^k}{\eta_0^k - \eta_0^{k-1}}, \tag{9}$$

where η_0^k are the parameter bifurcation values, was estimated for the first and the second bifurcation to be 4.60 in the map case and 5.9 in the PSGE case.

The main message of this paper is that chaotic motion in LJJs exists in the PSGE and in the map approach; qualitatively, the two approaches depict the same scenario. Other results of full PSGE integration will be published in a subsequent paper.

We wish to thank R.D. Parmentier for illuminating comments and for a critical reading of the manuscript. We had several interesting discussions with G. Costabile, S. Pagano, N.F. Pedersen, and M. Salerno, to whom goes our gratitude. This work is partly sponsored by the Progetto Finalizzato "Tecnologie Superconduttive e Criogeniche" of the Italian CNR.

References

[1] R.D. Parmentier, in: Solitons in action, eds. K. Lonngren and A. Scott (Wiley, New York, 1978) p. 173.
[2] G. Reinisch and J.C. Fernandez, Phys. Rev. B 25 (1982) 7352.
[3] M. Cirillo, J. Appl. Phys. 60 (1986) 338.
[4] R.L. Kautz, IEEE Trans. Magn. MAG-19 (1983) 465;
R.L. Kautz and R. Monaco, J. Appl. Phys. 57 (1985) 875.
[5] M. Octavio, Phys. Rev. B 29 (1984) 1231.
[6] A.R. Bishop, K. Fesser, P.S. Lomdahl, W.C. Kerr and S.E. Trullinger, Phys. Rev. Lett. 50 (1983) 1095.
[7] M. Cirillo, J. Appl. Phys., to be published.
[8] M. Salerno, M.R. Samuelsen, G. Filatrella, S. Pagano and R.D. Parmentier, Phys. Rev. B 41 (1990) 6641.
[9] M. Salerno, Phys. Lett. A 144 (1990) 453.
[10] G. Filatrella, G. Rotoli and R.D. Parmentier, Phys. Lett. A 148 (1990) 122.
[11] A. Davidson and N.F. Pedersen, Phys. Rev. B 41 (1990) 178.
[12] G. Rotoli, G. Costabile and R.D. Parmentier, Phys. Rev. B 41 (1990) 1958;
G. Costabile, R. Monaco, S. Pagano and G. Rotoli, Phys. Rev. B 42 (1990) 2651.
[13] D.W. McLaughlin and A.C. Scott, Phys. Rev. A 18 (1978) 1652.
[14] M. Scheuermann, J.T. Chen and J.J. Chang, J. Appl. Phys. 54 (1983) 3286.
[15] G. Costabile, R. Monaco and S. Pagano, J. Appl. Phys. 63 (1988) 5406;
G. Costabile, V.P. Koshelets, R. Monaco and S. Pagano, Japan. J. Appl. Phys. 26 (1987) 1639.
[16] G. Benettin, L. Galgani, A. Giorgilli and J.M. Strelcyn, Meccanica 15 (1980) 9.
[17] D. Ruelle, Chaotic evolution and strange attractors, Lezioni Lincee, Rome, May 1987 (Cambridge Univ. Press, Cambridge, 1989).
[18] D.A. Russel, J.D. Hanson and E. Ott, Phys. Rev. Lett. 45 (1980) 1175.
[19] W.H. Press, B.R. Flauvery, S.A. Teukolsky and W.T. Vetterlius, Numerical recipes (Cambridge Univ. Press, Cambridge, 1986).
[20] W.E. Milne, Numerical solutions of differential equations (Wiley, New York, 1953) ch. 2.
[21] G. Filatrella, N. Grønbech-Jensen, R. Monaco, S. Pagano, R.D. Parmentier, N.F. Pedersen, G. Rotoli, M. Salerno and M.R. Samuelsen, in: Proc. Workshop on Nonlinear superconductivity electronics and Josephson devices, Capri, September 1990, eds. G. Costabile, A. Davidson, S. Pagano, N.F. Pedersen and M. Russo (Plenum, New York), in press.